

Rapid fabrication of microhole array structured optical fibers

Rui Yang,¹ Yong-Sen Yu,^{1,3} Chao Chen,¹ Qi-Dai Chen,¹ and Hong-Bo Sun^{1,2,4}

¹State Key Laboratory on Integrated Optoelectronics, College of Electronic Science and Engineering, Jilin University, 2699 Qianjin Street, Changchun 130012, China

²College of Physics, Jilin University, 119 Jiefang Road, Changchun 130023, China

³e-mail: yuys@jlu.edu.cn

⁴e-mail: hbsun@jlu.edu.cn

Received August 1, 2011; accepted August 23, 2011;

posted September 2, 2011 (Doc. ID 152109); published September 27, 2011

A microhole array in a common single-mode fiber is fabricated by selective chemical etching of femtosecond-laser-induced fiber Bragg grating (FBG), which has a laser-modified region extending from the fiber core to the cladding–air boundary due to laser self-focusing. The shape and size of the orderly microhole on the fiber surface are controlled via changing conditions of FBG fabrication and chemical etching. A simultaneous sensing for surrounding refractive index and temperature is demonstrated by this microhole array FBG through measurement of the transmission power change and Bragg resonant wavelength shift. © 2011 Optical Society of America

OCIS codes: 060.2370, 060.3735, 060.4005.

Microstructures in an optical fiber, such as a microhole [1], a microchannel [2,3], or a microslot [4], can significantly change the features of light propagation or light–ambient matter interactions in a fiber, which have attracted a lot of interest recently. Microstructured fibers, such as photonic crystal fiber (PCF) [1,5], side-polished or D-shaped fiber (D-fiber) [6], and chemical etched thinned fiber (thinned fiber) [7,8], have been widely investigated for their applications in fiber telecommunications and fiber sensing. However, the relative complicated manufacturing process and high cost of PCF and D-fiber limit their extensive practical applications, while for thinned fiber, removal of the entire cladding or even some part of fiber core greatly reduces the fiber strength and durability. It is necessary to develop a simple, low-cost approach for introducing microstructures in common fibers. In recent years, femtosecond (fs) laser direct inscription in transparent and hard materials has attracted much attention due to the high spatial resolution and three-dimensional controllable micromachining [9,10]. Combined with the selective chemical etching of the laser-modified material, designed microstructures, for example, microchannels, have been realized in conventional single-mode fiber (SMF) [3]. Moreover, Zhou *et al.* reported on the fabrication of a microslot in a UV-written fiber Bragg grating (FBG) by additional chemically assisted fs laser direct writing [4]. This method is relatively simple and convenient to realize microstructures in low-cost conventional SMF, but point by point laser exposure to fabricate a modified region across the entire fiber is quite time consuming. In this Letter, we propose a method to fabricate a microhole array (MHA) in a SMF based on selective chemical etching of an FBG written by fs laser exposure under a phase mask [11,12]. The fs-laser-induced FBG has the modified grating regions extending from the fiber core to the cladding–air boundary, which are generated synchronously by fs laser self-focusing [13] during grating fabrication process. These laser-modified regions possess higher chemical activity, resulting in higher sensitivity to chemical etching than nonmodified regions (etching rate ratio

>100:1) [14]. So a fast selective etching in the laser-modified grating regions will be achieved when the fs-written FBG is immersed in etching solution, forming a microhole or microchannel array in fiber with the same period of grating. The generation of microhole does not need laser exposure to individual holes, greatly simplifying the fabrication process and reducing time and cost. The microstructures are highly repeatable and have potential for massive industrial production.

The schematic diagram of the setup for the fabrication of the FBG and the magnified grating region is shown in Fig. 1. In our experiments, a Ti:sapphire regenerative amplifier laser system (Spectra Physics) operating at 800 nm was adopted. The pulse duration was 100 fs, and the repetition rate was set at 1 kHz. The laser beam with 0.8 mJ pulse energy, which was adjusted by a neutral density

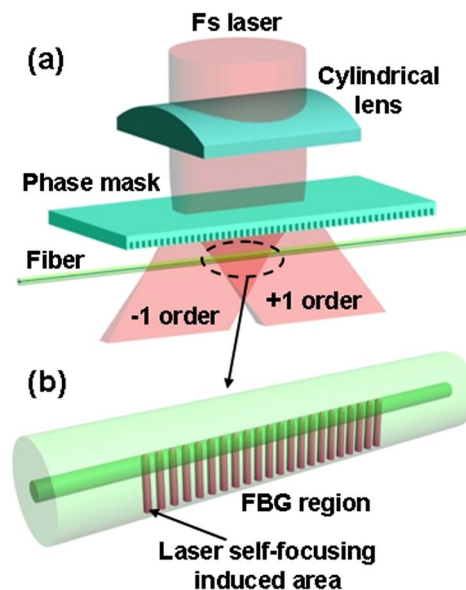


Fig. 1. (Color online) (a) Schematic diagram of the experimental setup for FBG fabrication by fs laser and phase mask. (b) The FBG region extending from fiber core to cladding–air boundary is magnified for clarity.

filter, was focused into the fiber sample (Corning SMF-28) via a cylindrical lens with focal length of 40 mm and passed through a phase mask with pitch of $3.33\ \mu\text{m}$. The space between the phase mask and fiber was about 3 mm to generate interference by the ± 1 -order diffractive laser beam [11]. The fiber was mounted onto a three-axis step motor and its two ends connected to a broadband light source (Superk Compact, NKT Photonics) and an optical spectrum analyzer (OSA) (AQ6370B, Yokogawa), respectively, to monitor the spectral change. The threshold power for the laser self-focusing effect inside the fiber is $0.4\ \text{mJ/pulse}$ in our experiment, and the corresponding light intensity is calculated to $6.4 \times 10^{12}\ \text{W/cm}^2$. An FBG with a length of 6.0 mm was attained after 3 s exposure with the fiber not moving parallel or perpendicular to the laser beam direction. The resonant wavelength λ_B is decided by the Bragg resonance equation $m\lambda_B = 2n_{\text{eff}}\Lambda_G$, where m is the order number, n_{eff} is the effective refractive index (RI) of the fiber mode, and the grating pitch Λ_G is one half of the phase mask period. A reflectivity of 96.8% located at 1604.4 nm, the third-order Bragg resonance, was observed in the OSA. The optical microscope images of the fiber grating structure before etching are shown in Figs. 2(a) and 2(b). The arrows denote laser beam direction. Obviously, the laser-modified grating area extends from the fiber core to the cladding–air boundary. The period of the grating is $1.665\ \mu\text{m}$, and the width of the modified region is about $3\ \mu\text{m}$.

To obtain the MHA, the fs-written FBG was immersed in a hydrogen fluoride (HF) aqueous solution with volume concentration of 4% at room temperature ($20\ ^\circ\text{C}$) to achieve selective corrosion. A typical transmission

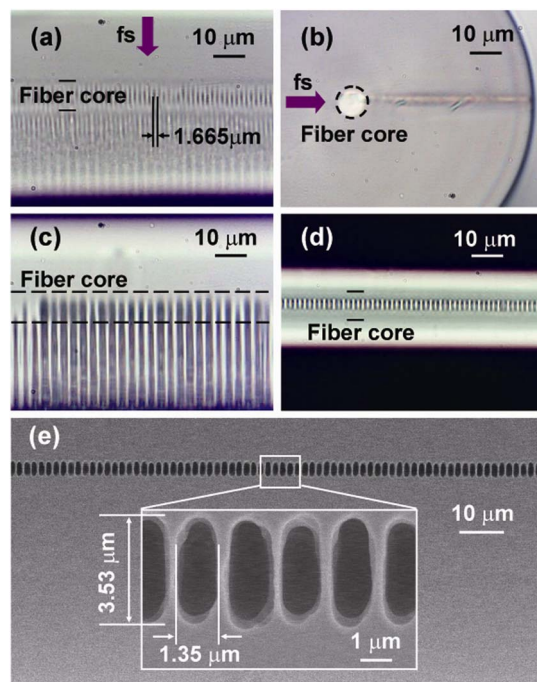


Fig. 2. (Color online) Microscope images of the fs-laser-induced FBG before and after chemical etching. (a) Side view normal to the beam axis and (b) cross section before etching. (c) Side view normal to the beam axis and (d) view from output side of laser beam after etching. (e) SEM image on the fiber grating surface after etching.

spectra change in chemical etching is shown in Fig. 3(a). A blueshift of the resonant wavelength and transmission loss begin after 30 min of chemical etching, which means most of the laser-modified region in the cladding has been eroded and the fiber core mode evanescent field is extending into the ambient acid solution. The etching solution has a smaller RI than the fiber cladding, causing the effective RI of the fiber core mode decrease and leading to the resonant wavelength blueshift. After 40 min of etching, the FBG was taken out of the HF acid and rinsed by a saturated sodium bicarbonate (NaHCO_3) solution to neutralize the acid. Then the grating was put into an ultrasonic water bath for 5 to 10 min to get rid of residual NaHCO_3 solution and debris that might be generated in etching. The etched fiber grating was observed under an optical microscope, and images of the grating structure are shown in Figs. 2(c) and 2(d). The microchannel array is clear in the side view of the fiber grating. Figure 2(d), viewed from the output direction of the laser beam, shows the MHA on the fiber surface. It is found from scanning electron microscope (SEM) images [Fig. 2(e)] that elliptical microholes are arranged in order with the period the same as the fiber grating's period. The major and the minor axes of the microhole are 3.53 and $1.35\ \mu\text{m}$, respectively, measured in the magnified figure in Fig 2(e).

If the chemical etching of fiber grating continues to 45 min, the microhole will be enlarged and finally connected to each other to form a microslot. The microslot will extend from the fiber surface into the fiber cladding with the etching process [Fig. 3(b)]. Meanwhile, the transmission power keeps falling along with the continued etching of the fiber core. The microslot extends into the cladding partly, and microchannels still exist deep inside the cladding. It is a state of microslot and microchannels coexisting in fiber. If the etching time is as long as 60 min, the microslot will cover the whole grating area without microchannels remaining [Fig. 3(c)], leading to the disappearance of Bragg resonance and a large transmission loss [Fig. 3(a)].

This MHA FBG may be used in optofluidics due to the microchannels for medium delivery and Bragg grating sensing of environmental medium RI. Experimentally,

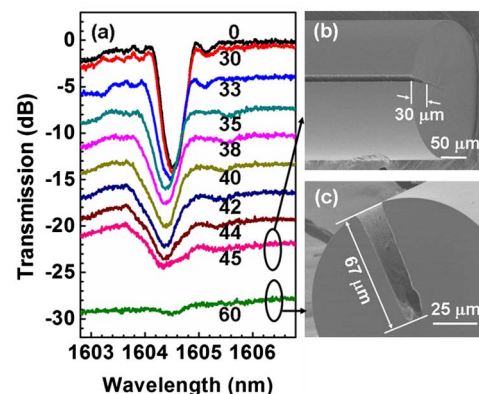


Fig. 3. (Color online) (a) Transmission spectra change of the FBG during the etching process. The numbers denote etching time in minutes. (b) SEM image of the microslot and microchannels coexisting in fiber after 45 min etching. (c) SEM image of the microslot in fiber after 60 min etching.

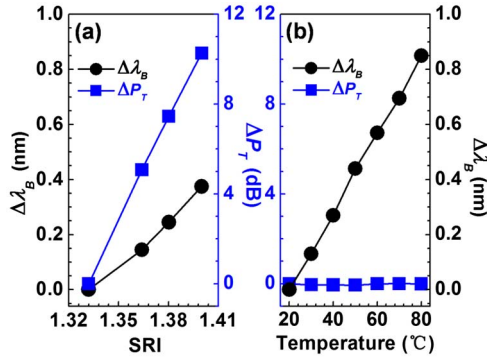


Fig. 4. (Color online) Bragg resonant wavelength shift ($\Delta\lambda_B$) and transmission power change (ΔP_T) in different environmental conditions. (a) Wavelength and power change with the SRI. (b) Wavelength and power change with temperature.

when the MHA FBG was immersed in different RI environments, the spectra changed in both resonant wavelength and transmission power [Fig. 4(a)]. The device was tested in glycerin aqueous solutions with different volume concentrations. The RIs of these glycerin solutions were measured by the Abbe refractometer at 589.3 nm and room temperature. The transmission spectra exhibit a redshift, and the power loss is reduced with increasing the surrounding refractive index (SRI). The relationship between the SRI (1.33–1.40) and the other two parameters (resonant wavelength and transmission power) are plotted in Fig. 4(a). The left y axis denotes Bragg resonant wavelength shift ($\Delta\lambda_B$), and the right one denotes transmission power change (ΔP_T) at the wavelength of 1605 nm. The circles and squares correspond to $\Delta\lambda_B$ and ΔP_T , respectively. From the function of Bragg resonant wavelength shift and the SRI, we can get the wavelength-SRI sensitivity of 5.484 nm/refractive index unit (RIU) in the RI range from 1.33 to 1.40. The minimal detectable change in the RI is 3.65×10^{-3} when the OSA resolution is 20 pm. For the case of transmission power change with a different SRI, the sensitivity is 151.347 dB/RIU. Furthermore, we measured the response of the MHA FBG to temperature in a furnace [Fig. 4(b)]. The transmission power variation is negligible with temperature, but the Bragg resonance is sensitive to it. The responsivity of Bragg resonant wavelength and transmission power to temperature are calculated to 0 nm/°C and 0.014 nm/°C, respectively. So this optofluidic device may be used to detect the SRI and temperature simultaneously. The relationship between these variables can be expressed in the form of matrix,

$$\begin{bmatrix} \Delta\lambda_B \\ \Delta P_T \end{bmatrix} = \begin{bmatrix} A1 & B1 \\ A2 & B2 \end{bmatrix} \begin{bmatrix} \Delta T \\ \Delta n_{\text{SRI}} \end{bmatrix},$$

where $A1$ and $A2$ are the temperature sensitivities for Bragg resonant wavelength and transmission power, respectively, while $B1$ and $B2$ are the SRI sensitivities

for them, respectively. Substituting the values obtained from experiments into the matrix, the final expression can be written as

$$\begin{bmatrix} \Delta\lambda_B \\ \Delta P_T \end{bmatrix} = \begin{bmatrix} 0.014 & 5.484 \\ 0 & 151.347 \end{bmatrix} \begin{bmatrix} \Delta T \\ \Delta n_{\text{SRI}} \end{bmatrix}.$$

Simultaneous sensing of the ambient RI and temperature is enabled through the measurement of the Bragg resonant wavelength shift and transmission power change of this MHA FBG.

In conclusion, we have proposed a method to fabricate an MHA FBG in common SMFs. The microhole or microchannel array in fiber is formed by selective chemical etching of the fs-laser-induced FBG, which has a laser-induced chemically active region extending from fiber core to cladding–air boundary. The shape and size of the microhole can be controlled through changing laser pulse energy and etching time. Simultaneous measurement for the SRI and temperature by this microstructured fiber device is demonstrated.

This work was supported by the “863” and “973” programs under grants 2009AA03Z401 and 2011CB013005, respectively, and by the National Natural Science Foundation of China (NSFC) under grants 60807030, 91123027, and 90923037.

References

1. C. M. B. Cordeiro, M. A. R. Franco, G. Chesini, E. C. S. Barretto, R. Lwin, C. H. B. Cruz, and M. C. J. Large, *Opt. Express* **14**, 13056 (2006).
2. A. van Brakel, C. Grivas, M. N. Petrovich, and D. J. Richardson, *Opt. Express* **15**, 8731 (2007).
3. Y. Lai, K. Zhou, L. Zhang, and I. Bennion, *Opt. Lett.* **31**, 2559 (2006).
4. K. Zhou, Y. Lai, X. Chen, K. Sugden, L. Zhang, and I. Bennion, *Opt. Express* **15**, 15848 (2007).
5. L. Rindorf and O. Bang, *J. Opt. Soc. Am. B* **25**, 310 (2008).
6. J. D. Gordon, T. L. Lowder, R. H. Selfridge, and S. M. Schultz, *Appl. Opt.* **46**, 7805 (2007).
7. W. Liang, Y. Huang, Y. Xu, R. K. Lee, and A. Yariv, *Appl. Phys. Lett.* **86**, 151122 (2005).
8. A. Iadicicco, A. Cusano, S. Campopiano, A. Cutolo, and M. Giordano, *IEEE Sens. J.* **5**, 1288 (2005).
9. J. F. Ku, Q. D. Chen, R. Zhang, and H. B. Sun, *Opt. Lett.* **36**, 2871 (2011).
10. Y. L. Zhang, Q. D. Chen, H. Xia, and H. B. Sun, *Nano Today* **5**, 435 (2010).
11. C. W. Smelser, S. J. Mihailov, and D. Grobncic, *Opt. Express* **13**, 5377 (2005).
12. C. Chen, Y. S. Yu, R. Yang, L. Wang, J. C. Guo, Q. D. Chen, and H. B. Sun, *J. Lightwave Technol.* **29**, 2126 (2011).
13. C. W. Smelser, D. Grobncic, and S. J. Mihailov, in *Quantum Electronics and Laser Science Conference (IEEE, 2005)*, Vol. 2, p. 1218.
14. C. Hnatovsky, R. S. Taylor, E. Simova, V. R. Bhardwaj, D. M. Rayner, and P. B. Corkum, *Opt. Lett.* **30**, 1867 (2005).